

Structural transformations in the Stranski-Krastanov growth of Mg on Mo(001)

M. C. Gallagher

Department of Physics, Lakehead University, Thunder Bay, Ontario, Canada P7B 5E1

M. S. Fyfield* and S. A. Joyce†

Environmental Molecular Sciences Laboratory, Pacific Northwest National Laboratory, Richland, Washington 99352

(Received 20 April 1998; revised manuscript received 21 July 1998)

The epitaxy of Mg, a hexagonal-closed-packed (hcp) metal in the bulk, onto a room-temperature body-centered-cubic Mo(001) substrate is investigated. A Stranski-Krastanov, layer by layer followed by islands, growth mode is observed including the initial stabilization of a metastable face-centered-cubic (fcc) phase of Mg. Layer by layer growth persists for four layers. During growth of the first and second layer the highly corrugated surface potential and lattice mismatch both act to limit island size, and growth proceeds via nucleation and growth of small two-dimensional islands. Third- and fourth-layer growth proceeds by step flow. The increase in the diffusion constant necessary for step flow may be aided by the presence of a stress relieved $c(2 \times 2)$ surface reconstruction in this regime. The reconstruction may result from a buckling of the Mg lattice to conform to the smaller Mo(001) spacing. Measurement of atomic step heights confirms the growth of fcc Mg(001). Beyond four layers a transition to three-dimensional (3D) island growth occurs. Associated with this transition is a change in crystal structure. The 3D islands exhibit hexagonal symmetry with two domains rotated by 30° with respect to one another. Measurement of emergent screw dislocations at the surface of the islands confirms the growth of hcp Mg(0001). Evidence of edge dislocations aligned with steps in the underlying Mo substrate are also observed. [S0163-1829(98)03147-6]

I. INTRODUCTION

The epitaxial growth of thin films on solid substrates continues to attract a great deal of interest. Many modern technologies rely on the fabrication of ultrathin, atomically structured layers. Often the interfacial strain involved in heteroepitaxy can be exploited to grow metastable phases of metals that exhibit physical and chemical properties which differ from those of the bulk material. Progress in the growth of these films is ultimately related to an improved understanding of the microscopic processes involved in growth. The advent of scanning tunneling microscopy (STM) has provided the unprecedented ability to investigate the underlying atomic processes involved in epitaxial growth.

In this paper we study the room-temperature growth of magnesium metal on the Mo(001) surface. The (001) surface of the bcc metals is highly corrugated and the activation energy for the surface diffusion of adsorbed species is high compared with the close-packed faces. The adsorbate-surface interaction tends to dominate initial film growth, and growth of the first two or three layers on these surfaces is generally pseudomorphic.¹ The lattice parameter of Mo (3.15 Å) compares favorably with Mg nearest-neighbor separation (3.21 Å). Previous low-energy electron diffraction (LEED) experiments report pseudomorphic growth of Mg on Mo(001) at low coverage and a transition to films with hexagonal symmetry at higher coverage.² Using STM we identify the pseudomorphic film as metastable fcc Mg. The fcc growth proceeds layer by layer for four layers. Beyond four layers strain relief is accomplished by a simultaneous transition to three-dimensional island growth and the growth of hcp Mg(0001).

II. EXPERIMENT

The experiments were performed in a UHV chamber with facilities for Auger electron spectroscopy (AES) and STM. The STM and control electronics are both commercially available.³ Measurements were made using etched W and mechanically cut Pt-Ir tips cleaned *in situ* using field emission techniques. STM data are presented as gray scales with intensity representing absolute tip height or in the case of derivative mode, the curvature of the surface. In order to perform LEED measurements the STM instrument was removed and LEED optics installed in the chamber.

The Mo(001) crystal was cleaned by repeated cycles of annealing at 1300 K in 5×10^{-8} Torr of oxygen followed by a flash to 2000 K. All temperatures were measured using an optical pyrometer assuming an emissivity of 0.3. This cleaning procedure yields surfaces with large terraces, many in excess of 1000 Å wide. The terraces are separated by single height atomic steps (1.6 Å high). No multiple height steps are observed. Steps at different regions of the surface have no preferred orientation (no nominal miscut of sample); however, they are comprised of step edges oriented along $\langle 100 \rangle$ directions. Each terrace exhibits a high degree of perfection. Adatom islands or vacancy islands are never observed.

The films were grown by evaporating Mg metal from a ribbon source at a rate of 0.8–5 ML/min. The sample was nominally at room temperature for all depositions. Mg coverages were determined by direct comparison with previously published Auger peak heights;² further calibration was provided by direct STM observation of Mg epitaxy. Due to interference from low-energy Mo Auger peaks, we were unable to measure coverage of less than 0.35 ML in AES.

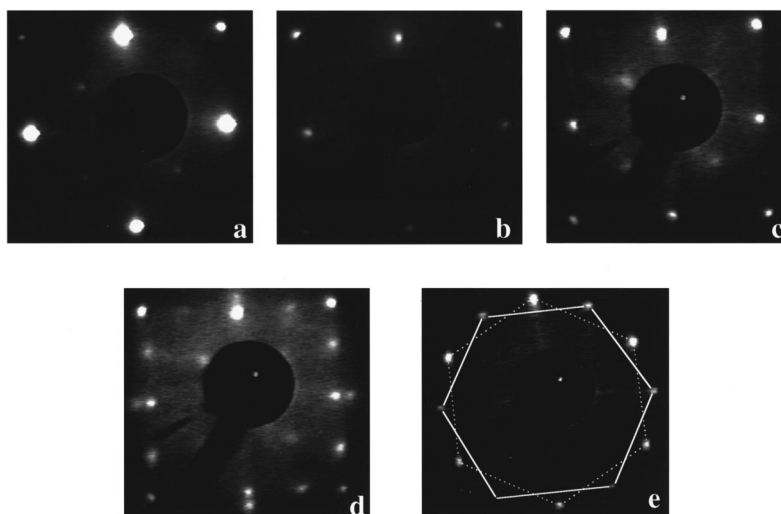


FIG. 1. LEED as a function of Mg coverage. The nominally clean Mo(001) surface exhibits a weak $c(2 \times 2)$ symmetry (a). Deposition of one layer of Mg produces a 1×1 pattern (b). With further deposition of up to four layers the $c(2 \times 2)$ pattern redevelops (c). LEED after five layers is a superposition of the $c(2 \times 2)$ pattern with a two domain hexagonal pattern (d). For thick films a two-domain hexagonal pattern with additional streaking along $\langle 100 \rangle$ is observed (e).

III. RESULTS AND DISCUSSION

A. LEED

Previous LEED measurements report pseudomorphic growth of Mg and the appearance of a hexagonal pattern at five layers.² Figure 1 illustrates the evolution of the LEED pattern during Mg deposition. The nominally clean Mo(001) surface exhibits an extremely weak $c(2 \times 2)$ pattern. Oxygen, carbon, sulfur, and hydrogen adsorption on Mo(001) can produce $c(2 \times 2)$ overlayers.⁴⁻⁸ Auger spectra reveal no O, C, or S within the detection limit, and studies by others indicate that the hydrogen-induced $c(2 \times 2)$ phase is not stable at room temperature.⁸ This $c(2 \times 2)$ pattern disappears with initial Mg deposition leaving a (1×1) pattern; however, with increasing thickness a $c(2 \times 2)$ pattern develops. The bulk Mg-Mg separation is 3.21 \AA , somewhat larger than the nearest-neighbor separation of 3.15 \AA for the Mo(001) surface. A reduction of stress in the film, and conservation of the Mg-Mg bond length with the in-plane lattice constant of 3.15 \AA can be attained by buckling of the Mg overlayer (Fig. 2) in a manner consistent with the symmetry observed in LEED.

In agreement with Wu *et al.*,² the growth of Mg with hexagonal symmetry is observed after four layers. The LEED pattern consists of a superposition of the original $c(2 \times 2)$ pattern and two hexagonal patterns each rotated by 30° . For increasingly thick films the $c(2 \times 2)$ contribution is diminished. At an approximately 12-layer equivalent exposure, only the two domain hexagonal pattern remains with some additional streaking along $\langle 100 \rangle$ directions of the substrate. The alignment of the hexagonal surface domains with the square $\langle 100 \rangle$ substrate is shown schematically in Fig. 1(e). The hexagonal spots are all of roughly equal intensity, suggesting that there is no “global” preference for one domain over the other. Based on the diffraction alone, a distinction between the sixfold symmetric hcp (001) and the threefold symmetric fcc (111) surfaces is not possible due to

the multiple domain growth. As will be shown below, for this system, scanning tunneling microscopy can be used to distinguish these surfaces.

B. STM

Initial two layers

Figure 3 represents a Mg coverage below the detectable AES limit. The image shows two Mo(001) terraces separated

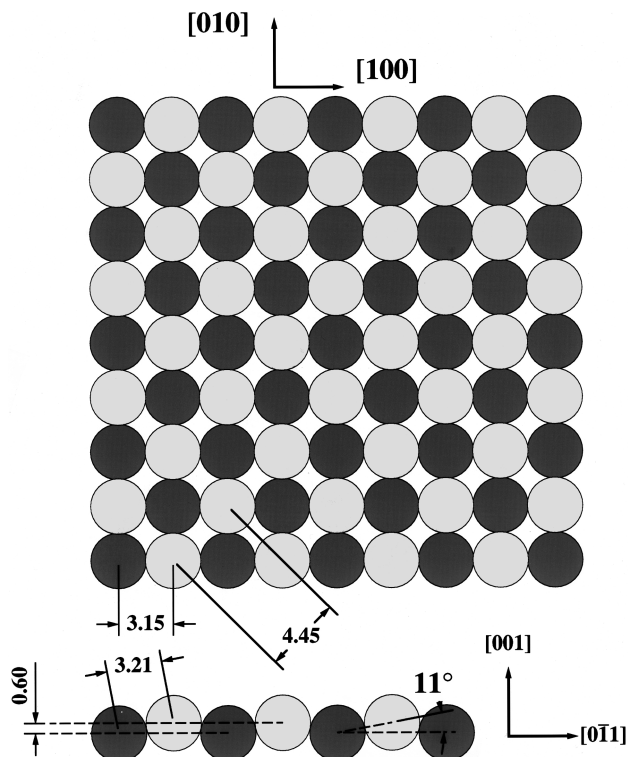


FIG. 2. Buckling of the pseudomorphic Mg layer on Mo(001) preserves the Mg-Mg bond length and produces a $c(2 \times 2)$ superstructure as observed in LEED.

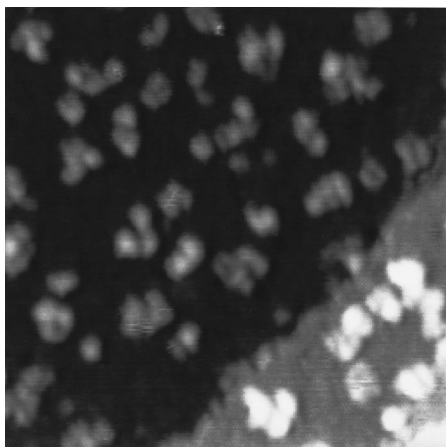


FIG. 3. A $400 \times 400 \text{ \AA}$ STM image of a submonolayer Mg film on Mo(001). For the first two layers growth proceeds via the nucleation and growth of a high density of small 2D islands.

by a single height atomic step. In addition, 2D Mg islands are dispersed about each terrace. Increasing coverage produces a higher density of small islands of the order of 50–60 Å in diameter, which persist until completion of the initial layer. 2D growth of second layer Mg also proceeds by island nucleation. The small islands show no evidence of a $c(2 \times 2)$ reconstruction.

Temperature programmed desorption (TPD) indicates the binding energy for monolayer Mg on Mo(001) is up to twice the bulk Mg value.² This reflects the corrugated nature of the bcc (001) surface and limits the mobility of Mg adatoms. Limited mobility promotes island nucleation on terraces rather than step flow growth.⁹ In the absence of strain, the saturation island density is $N \sim (r/h_0)^{1/3}$,¹⁰ where r is the deposition rate and h_0 is the hopping rate. The films exhibit a dimensionless saturation Mg island density (number of islands/unit cell) of $5 \pm 2 \times 10^{-3}$. The lattice mismatch between the Mg layer and the Mo surface can also limit island size. Strain relief in heteroepitaxial systems favors the growth of small islands.¹¹ When the Mg flux was varied by a factor of 6, no systematic variation in the island size was observed. However, more experiments are needed where the substrate temperature, and hence the hopping rate, is varied to determine whether the small island size results from the growth kinetics or from the interfacial stress.

fcc magnesium

Following completion of the second layer, the mobility of Mg adatoms in the third layer is sufficiently high and growth proceeds by step flow. In this regime the diffusion length is in excess of the terrace width, which in many cases exceeds 1000 Å. LEED indicates growth remains pseudomorphic. Figure 4 shows an STM image of a 2.6-layer-thick film. The growth of new terraces out from existing step edges is clear. On closer examination, the step structure shown in Fig. 4 displays an unusual characteristic. On going from left to right, the steps up are $\sim 2.1 \text{ \AA}$ high, whereas the steps down are only 0.5 \AA . It is further noted that a step up is always followed by a step down. The height difference between an up step and a down step is 1.6 \AA , the minimum step height on Mo(001). These results show that the Mg grows with a

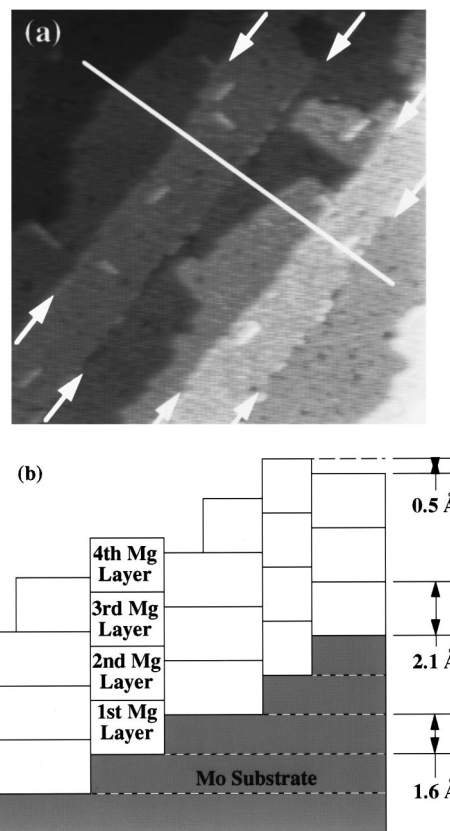


FIG. 4. A $1000 \times 1000 \text{ \AA}$ image of a 2.7-layer Mg film on Mo(001). Growth proceeds by step flow out from Mo steps (arrows). The 2.1-\AA step height indicates the growth of fcc Mg and produces a 0.5-\AA offset at Mo steps.

structure that has a step height of 2.1 \AA . The LEED results, on the other hand, show that the growth is pseudomorphic and as such the nearest-neighbor separation (d_{nn}) in the surface is the same as the Mo(001), i.e., 3.15 \AA . For bcc (001) surfaces, the step height is $d_{nn}/2$. For fcc (001), however, the step height is $d_{nn}/\sqrt{2}$, which for $d_{nn} = 3.15 \text{ \AA}$ corresponds to a step height of 2.2 \AA , in good agreement with the observation. We therefore conclude that the Mg, at least for the first four layers, grows with a fcc structure. This offset is only observed for films in excess of two layers.

An abnormal fcc phase of Mg was previously observed during the initial stages of Mg epitaxy on MgO(001).¹² Similar to Mo(001), growth was dictated by the symmetry of the substrate; however, unlike Mo, the fcc phase on MgO grew as three-dimensional islands rather than as a 2D film.

An increased adatom mobility with increasing film thickness has been reported for Ni epitaxy on Ru(0001).¹³ In this case the increased mobility was ascribed to successive relaxation of lattice strain in the film with thickness. The evolution of the 0.5-\AA offset with Mg thickness suggests relaxation normal to the surface. The relaxation may result in increased mobility and also explain the transition to step flow growth. In addition, stress relief may be accomplished by the development of the stress relieved $c(2 \times 2)$ surface reconstruction. Each magnesium terrace in Fig. 4 is a mosaic of small domains separated by dark lines. Within each domain (not shown) the surface exhibits $c(2 \times 2)$ symmetry consistent with the superstructure observed in LEED. A phase shift

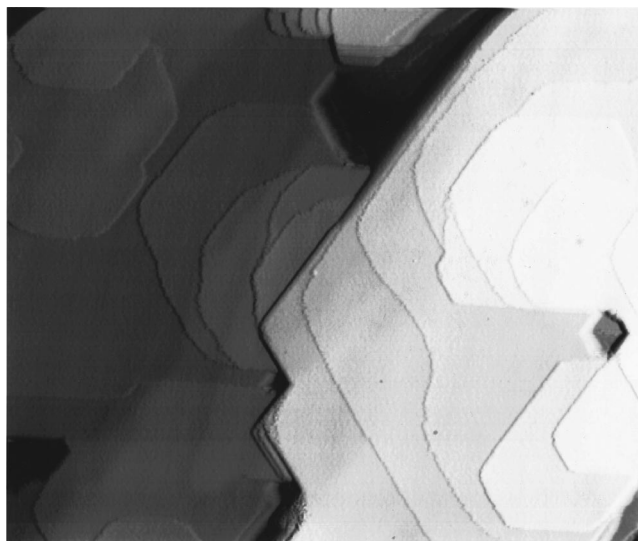


FIG. 5. A $2000 \times 2000 \text{ \AA}$ STM image obtained following deposition of a thick Mg film on Mo(001). The surface is covered with 3D Mg islands with hexagonal symmetry.

in the $c(2 \times 2)$ structure with respect to the underlying lattice produces the observed domain structure.

Hexagonal islands

The layer by layer growth of fcc magnesium persists until completion of the fourth layer. Beyond four layers there is a transition to 3D island growth on top of the existing pseudomorphic film. Still further deposition results in island coalescence; however, even the thickest films studied (>50 layer equivalent) exhibited deep holes and exposed fcc Mg.

Accompanying the transition to 3D growth is a change in crystal structure. Figure 5 is an image of a thick magnesium film. With the exception of a few deep holes, three-dimensional islands cover the surface. The islands exhibit hexagonal symmetry with two possible orientations each rotated by 30° with respect to one another. As noted above, this hexagonal structure could result from either a fcc(111) or an hcp(0001) surface. An unambiguous determination of the structure is provided by the nature of defects at the surface.

Figure 6 is an image of a 3D island. In evidence are

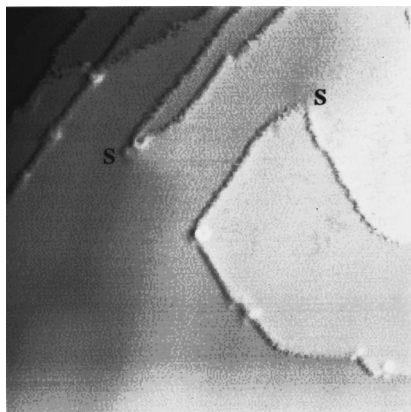


FIG. 6. A STM image of S at the surface of a 3D island. Presented in derivative mode to highlight steps, all screw dislocations produce two monatomic steps and indicate the growth of Mg(0001).

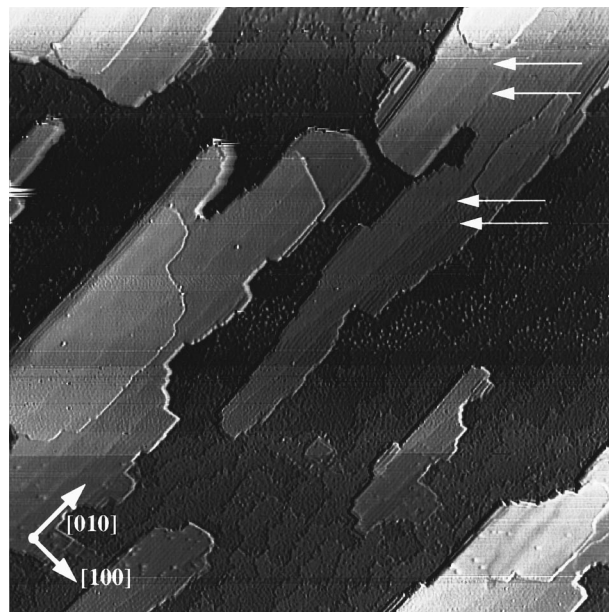


FIG. 7. A $3000 \times 3000 \text{ \AA}$ image presented in derivative mode following 4.4-layer equivalent exposure. The transition to 3D island growth is evident. Lines at the surface of the islands (arrows) running along the $[100]$ direction are associated with subsurface edge dislocations in the Mg film. Some islands also exhibit long-range reconstruction.

several emergent screw dislocations (S). When screw dislocations intersect the surface they generate steps that emerge from otherwise flat terraces. In all cases, we observe two atomically high steps emerging from the screws and a Burgers vector of 5.2 \AA . Due to stacking requirements the screw dislocations in a hcp material must produce steps in multiples of two atomic heights, whereas fcc materials would require steps in multiples of three. These results eliminate the possibility of fcc (111) islands and confirm the growth of bulklike hexagonal close-packed structures.

Screw dislocations are observed on all of the large three-dimensional islands. Growth via screw dislocations indicates that diffusion is not a rate-limiting step,¹⁴ and growth is proceeding under conditions of low supersaturation and the structures are near equilibrium.

The islands also show evidence of subsurface edge dislocations. These dislocations are identified by localized changes in the height of an otherwise flat terrace. The magnitude of the change is always a fraction of the monatomic step height. In differential mode, Fig. 7, the changes show up as lines extending across the island (arrows). At the perimeter of the islands the lines run into steps in the underlying Mo substrate. The origin of these dislocations can be understood if we consider the 0.5-\AA offset that occurs between pseudomorphic Mg layers on adjacent Mo terraces. If a 3D hexagonal island straddles adjacent Mo terraces, the 0.5-\AA offset produces an edge dislocation at the base of the island.

Figure 8(a) is another STM image taken on top of an hexagonal island. The step height at the perimeter is $\approx 12 \text{ \AA}$ high (lower left-hand corner) whereas the step height between two adjacent terraces on the island is $\approx 2.6 \text{ \AA}$ (monatomic hcp step). The step has a frizzy appearance indicating motion of the step. Motion is caused by the attachment and detachment of Mg adatoms at the step edge on a time scale

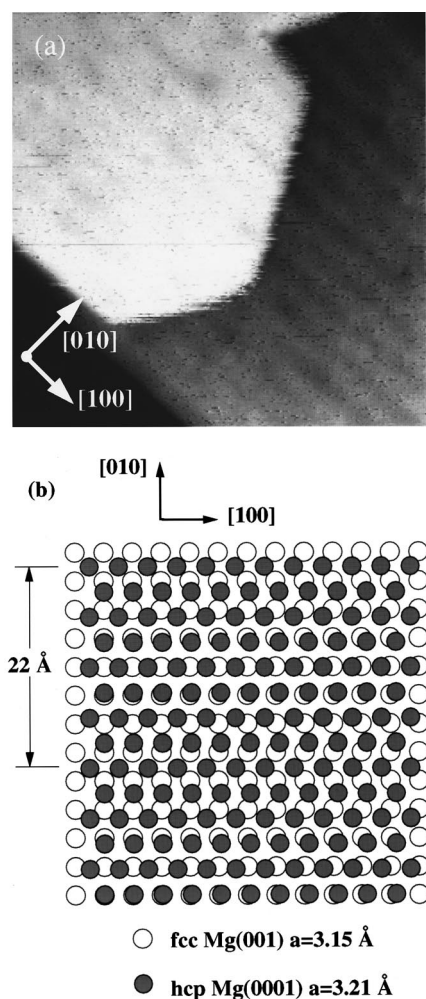


FIG. 8. A STM image of the surface of a 3D island (a). The 23-Å spacing between the parallel lines in the image is similar to the 22-Å coincidence between fcc Mg(001) and Mg(0001) along [010] (b).

faster than STM image acquisition.¹⁵ On the island a weak superstructure is also evident. Lines spaced 23 Å apart extend the length of the island. The lines run along the $\langle 100 \rangle$ directions of the substrate, and are most evident on islands a few layers thick becoming weaker with increasing island thickness (see, for example, Fig. 7).

From LEED we know the islands are oriented with respect to the fcc film such that $\langle 0001 \rangle \parallel \langle 001 \rangle$ and $\langle 10\bar{1}0 \rangle \parallel \langle 110 \rangle$. Using a bulk lattice constant of 3.21 Å for the island, and 3.15 Å for the pseudomorphic fcc film, this produces a coincidence of about seven lattice spacings along

$\langle 010 \rangle$ or ≈ 22 Å [Fig. 8(b)]. Thus the lines seen in the STM and the streaking observed in the LEED are produced by a coincidence between the fcc and hcp lattice along the $\langle 100 \rangle$ directions.

IV. SUMMARY

The corrugated nature of the bcc (001) surface is sufficient to stabilize the growth of pseudomorphic fcc Mg. The fcc film consists of small domains with local $c(2 \times 2)$ symmetry. The $c(2 \times 2)$ symmetry may be produced by buckling of the Mg layer in an effort to relieve stress and preserve the equilibrium Mg bond length while at the same time maintaining pseudomorphic registry with the substrate. The strain energy limits the pseudomorphic thickness to four layers. Beyond four layers the growth of Mg(0001) is observed. As a result the onset mode can be described as Stranski-Krastanov.⁹ The fcc layer grows in a layer by layer fashion, while the onset of Mg(0001) is accompanied by a simultaneous transition to 3D island growth.

Growth of the first two layers proceeds by the nucleation of a high density of small 2D islands of between 50 and 60 Å in diameter. The third and fourth layers grow by step flow. The transition to step flow is consistent with previous TPD indicating Mg binds more strongly to Mo than to itself.² The increase in the surface diffusion constant may result from relaxation of lattice strain with increasing film thickness.^{13,16} Stress relief may also be accomplished by the development of a $c(2 \times 2)$ surface reconstruction in the growing film.

Identification of the film structure at various stages of growth was provided by STM characterization of atomic defects. Analysis of step heights identified the growth of fcc Mg(001). Screw dislocations at the surface with a Burgers vector of 5.2 Å confirmed growth of Mg(0001) rather than fcc Mg(111) islands. The 3D islands also exhibited edge dislocations produced by the 0.5-Å misfit between adjacent Mg terraces in the underlying pseudomorphic film.

ACKNOWLEDGMENTS

This research was supported by the U.S. Department of Energy, Office of Basic Energy Sciences, Division of Materials Science. Pacific Northwest National Laboratory is a multiprogram national laboratory operated for the U.S. Department of Energy by Battelle Memorial Institute under Contract No. DE-AC06-76RLO 1830. One of the authors (M.C.G.) would like to acknowledge financial support from the National Science and Engineering Research Council (NSERC) of Canada.

*Permanent address: Portland State University, ESR/Physics, Portland, Oregon 97207.

†Author to whom correspondence should be addressed. FAX: +1 509 376-6066. Electronic address: sa.joyce@pnl.gov

¹E. Bauer, Appl. Surf. Sci. **11/12**, 479 (1982).

²M.-C. Wu *et al.*, J. Vac. Sci. Technol. A **10**, 1457 (1992).

³Scanning Head: McAllister Technical Services. Control Electronics: RHK Technologies.

⁴C. Zhang *et al.*, Surf. Sci. **164**, L835 (1985).

⁵C. Guillot, R. Riwan, and J. LeCante, Surf. Sci. **59**, 581 (1976).

⁶E. Ko and R. J. Madix, Surf. Sci. **100**, L449 (1980).

⁷L. J. Clarke, Surf. Sci. **102**, 331 (1981).

⁸P. J. Estrup, J. Vac. Sci. Technol. **16**, 635 (1979).

⁹*Kinetics of Ordering and Growth at Surfaces*, edited by M. G. Lagally (Plenum, New York, 1990).

¹⁰G. S. Bales and D. C. Chrzan, Phys. Rev. B **50**, 6057 (1994).

¹¹C. Ratch, A. Zangwill, and P. Smilauer, Surf. Sci. **314**, L937 (1994).

¹²A. P. Janssen, R. C. Schoonmaker, and A. Chambers, Surf. Sci. **49**, 143 (1975).

¹³J. A. Meyer, P. Schmid, and R. J. Behm, Phys. Rev. Lett. **74**, 3864 (1995).
¹⁴W. K. Burton, N. Cabrera, and F. C. Frank, Philos. Trans. R. Soc. London, Ser. A **243**, 299 (1951).

¹⁵J. F. Wolf, B. Vicenzi, and H. Ibach, Surf. Sci. **249**, 233 (1991).
¹⁶J. H. van der Merwe, D. L. Tönsing, and P. M. Stoop, Surf. Sci. **312**, 387 (1994).